

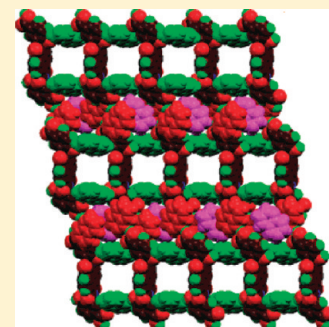
Solid State Assemblies of Cyclic Imides Tethered Hydroxy Benzoic Acids with Pyridine and Quinoline: Toward the Formation of Channels and Cavities

Devendra Singh and Jubaraj B. Baruah*

Department of Chemistry, Indian Institute of Technology Guwahati, Guwahati 781 039 Assam, India

S Supporting Information

ABSTRACT: A series of inclusion compounds of different cyclic imides tethered hydroxybenzoic acid hosts (1–8) with guests pyridine (I–IV) and quinoline (V–X) have been prepared and structurally characterized. Supramolecular aspects pertaining to the influence of guest molecules toward the formation of solid state network structures of hosts are described. Hydrogen bonding of both carboxylic acid and hydroxyl groups as well as $\pi\cdots\pi$ stacking of aromatic imide units led to the formation of channels of different dimensionalities in the supramolecular architectures of I–X. In these structures, the channels are occupied by the guest molecules that interact with both hydrogen bonding groups of host molecules via different types of hydrogen bond motifs. Thermogravimetric analyses correspond to the association of different numbers of guest pyridine or quinoline molecules with isomeric hydroxybenzoic acid hosts. Solid state fluorescence spectra of hosts 1–8 are recorded which show emissions in the region of 412–516 nm. Overall this structural study represents the combined effects of π -stacking aromatic imide synthons and two hydrogen bonding carboxylic acid and hydroxyl functional groups in the presence of aromatic nitrogen containing guests to create fascinating supramolecular architectures.



INTRODUCTION

The directional properties of weak interactions are useful in construction of self-assemblies.¹ Hydroxyl and carboxylic acid groups are the commonly used functional groups to construct self-assemblies.² The combination of hydroxyl and carboxylic acid groups in aromatic compounds has been very useful in making useful supramolecular assemblies.³ However, complicity in such system can be enhanced by adding other functional groups such as imide groups that have also been used as versatile scaffolds to design the new host–guest systems.⁴ Cyclic imides attached to aromatic rings possess a dipolar nature, and this effect provides extra stability to the packing arrangement.⁵ From this point of view, imides containing π -stacking synthons such as naphthalimides or naphthalene diimides combined with carboxylic acid or hydroxyl functional groups draw special interest.⁶ These multifunctional molecules create extended network solids by self-assembly through hydrogen bonding interactions of the functional groups along with the $\pi\cdots\pi$ stacking interactions of the naphthalimide rings. Recently, Reger et al. have studied supramolecular structural features of organic network solids as well as metal–organic framework (MOF) type architectures derived from bifunctional molecules that contained both a carboxylic acid and a $\pi\cdots\pi$ stacking naphthalimide synthon, indicating the importance and versatility of this supramolecular synthon.⁷

Besides that, supramolecular assemblies of hydroxyl group containing compounds such as alcohols, phenols, and carboxylic acids with pyridine or related nitrogen containing aromatic compounds are well studied.⁸ Some of these either lead to co-crystals or ionic salts which are useful in

pharmaceutical chemistry⁹ as well as in the synthesis of porous materials.¹⁰ In our recent reports, we have shown different types of hydrogen bond motifs in inclusion compounds of pyridine and quinoline with various bifunctional molecules that contained both carboxylic acid group and aromatic imide π -stacking unit.^{11a,b} The structural investigation of few solvates of other bifunctional molecules in which aromatic hydroxyl groups are tethered by phthalimide and pyromellitic diimide units have also shown interesting supramolecular architectures.^{11c}

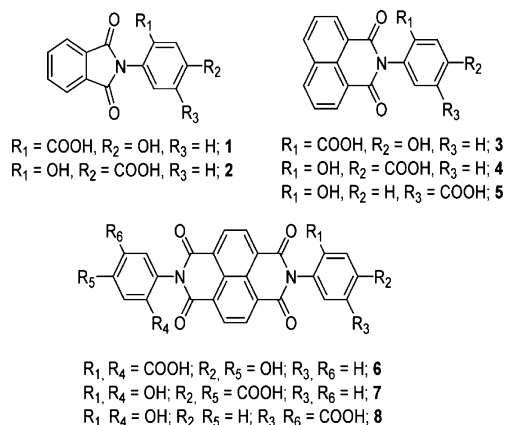
However, there is no systematic study carried out to ascertain the role of directional interactions and the type of assemblies that can be formed from trifunctional molecules containing both hydroxyl and carboxylic acid groups tethered by a π -stacking imide synthon. For this purpose we have chosen a few phthalimide, naphthalimide, and naphthalene diimide derivatives (Scheme 1) in which the carboxylic acid and hydroxyl groups are attached at different positions of the aromatic ring and studied the structures of their pyridine and quinoline inclusion compounds. Such a study will not only provide information on the assembling process but will also be able to distinguish the deprotonation processes of the hydroxyl or carboxylic acid groups to form their corresponding salt. Further, analogous naphthalimide derivatives as used in this study have interesting molecular recognition properties¹² and will provide a guideline on the formation of assemblies by such derivatives.

Received: March 13, 2012

Revised: May 7, 2012

Published: May 8, 2012

Scheme 1. Structures of Host Molecules



EXPERIMENTAL SECTION

Structure Determination. The X-ray single crystal diffraction data were collected at 296 K with MoK α radiation ($\lambda = 0.71073 \text{ \AA}$) using a Bruker Nonius SMART CCD diffractometer equipped with a graphite monochromator. The SMART software was used for data collection and also for indexing the reflections and determining the unit cell parameters; the collected data were integrated using SAINT software. The structures were solved by direct methods and refined by full-matrix least-squares calculations using SHELXTL software.¹³ All the non-H atoms were refined in the anisotropic approximation against F^2 of all reflections. The H-atoms, except those attached to nitrogen and oxygen atoms, were placed at their calculated positions and refined in the isotropic approximation. The H-atoms attached to nitrogen and oxygen atoms were located in the difference Fourier maps and refined with isotropic displacement coefficients in the structures I, II, IV, V, VII, VIII, and X, whereas the H-atoms of O–H and N–H groups were constrained in the case of structures III, VI, and IX. The disordered guest pyridine or pyridinium and quinoline molecules were refined by sharing two nitrogen atoms with two carbon atoms having half occupancies at two opposite sites. Crystallographic data collection was done at room temperature and the data are tabulated in Table 1.

Synthesis and Characterization of Compounds and Their Solvates/Salts/Cocrystal. 2-(1,3-Dioxo-1,3-dihydro-isoindol-2-yl)-5-hydroxy-benzoic acid (**1**): A solution of phthalic anhydride (0.740 g, 5 mmol) and 2-amino-5-hydroxy-benzoic acid (0.765 g, 5 mmol) in acetic acid (15 mL) was refluxed for 3 h. The reaction mixture was cooled to room temperature, poured into ice cooled water (30 mL), and kept for three days. Colorless crystals of the product were obtained. Yield: 87%; IR (KBr, cm^{-1}): 3274 (m), 1714 (s), 1615 (s), 1505 (m), 1463 (s), 1386 (s), 1336 (m), 1289 (s), 1241 (s), 1135 (m), 1108 (m), 933 (w), 884 (m), 843 (m), 793 (w), 749 (w), 719 (m), 685 (w). $^1\text{H NMR}$ (400 MHz, $\text{DMSO-}d_6$): 10.22 (s, 1H), 7.95 (dd, 2H, $J = 6.0 \text{ Hz}$), 7.88 (dd, 2H, $J = 3.2 \text{ Hz}$), 7.45 (s, 1H), 7.32 (d, 1H, $J = 8.4 \text{ Hz}$), 7.12 (d, 1H, $J = 8.4 \text{ Hz}$). ESI-MS: 284.115 $[\text{M} + \text{H}^+]$.

4-(1,3-Dioxo-1,3-dihydro-isoindol-2-yl)-3-hydroxy-benzoic acid (**2**): A solution of phthalic anhydride (0.740 g, 5 mmol) and 4-amino-3-hydroxy-benzoic acid (0.765 g, 5 mmol) in acetic acid (10 mL) was refluxed for 3 h. The reaction mixture was cooled to room temperature, poured into ice cooled water (30 mL), and stirred for 15 min. A brown colored crystalline material of the product was obtained. This was filtered and dried in open air. Yield: 84%; IR (KBr, cm^{-1}): 3388 (s), 1732 (s), 1694 (s), 1599 (m), 1388 (s), 1289 (w), 1245 (m), 1208 (m), 1124 (m), 1103 (m), 1075 (m), 949 (w), 884 (m), 764 (w), 714 (m), 588 (w). $^1\text{H NMR}$ (400 MHz, $\text{DMSO-}d_6$): 10.31 (s, 1H), 7.98 (dd, 2H, $J = 3.2 \text{ Hz}$), 7.91 (dd, 2H, $J = 3.2 \text{ Hz}$), 7.56 (s, 1H), 7.50 (d, 1H, $J = 8.4 \text{ Hz}$), 7.40 (d, 1H, $J = 8.4 \text{ Hz}$). ESI-MS: 284.056 $[\text{M} + \text{H}^+]$.

2-(1,3-Dioxo-1H,3H-benzo[de]isoquinolin-2-yl)-5-hydroxy-benzoic acid (**3**): A solution of 1,8-naphthalic anhydride (0.990 g, 5 mmol) and 2-amino-5-hydroxy-benzoic acid (0.765 g, 5 mmol) in *N,N*-

dimethylformamide (15 mL) was refluxed for 5 h. The reaction mixture was cooled to room temperature, poured into ice cooled water (50 mL), and stirred for 15 min. A brown colored precipitate of the product was formed, which was filtered and air-dried. Yield: 86%; IR (KBr, cm^{-1}): 3293 (s), 1720 (s), 1693 (s), 1623 (m), 1582 (s), 1499 (w), 1382 (m), 1293 (m), 1250 (s), 1208 (s), 824 (w), 780 (m), 665 (w). $^1\text{H NMR}$ (400 MHz, $\text{DMSO-}d_6$): 10.07 (s, 1H), 8.49 (m, 4H), 7.89 (t, 2H, $J = 8.0 \text{ Hz}$), 7.48 (s, 1H), 7.26 (d, 1H, $J = 8.4 \text{ Hz}$), 7.10 (d, 1H, $J = 8.4 \text{ Hz}$). ESI-MS: 334.127 $[\text{M} + \text{H}^+]$.

4-(1,3-Dioxo-1H,3H-benzo[de]isoquinolin-2-yl)-3-hydroxy-benzoic acid (**4**): Compound **4** was also obtained by the cyclo-condensation reaction of 1,8-naphthalic anhydride and 4-amino-3-hydroxy-benzoic acid with the similar procedure as used for **3**. Yield: 84%; IR (KBr, cm^{-1}): 3397 (m), 1774 (w), 1737 (m), 1693 (s), 1651 (s), 1621 (s), 1589 (s), 1513 (w), 1437 (m), 1379 (m), 1358 (m), 1302 (w), 1270 (w), 1243 (s), 1121 (m), 1012 (w), 960 (w), 893 (w), 784 (m), 764 (m). $^1\text{H NMR}$ (400 MHz, $\text{DMSO-}d_6$): 10.11 (s, 1H), 8.51 (m, 4H), 7.90 (t, 2H, $J = 7.6 \text{ Hz}$), 7.56 (s, 1H), 7.50 (d, 1H, $J = 8.0 \text{ Hz}$), 7.10 (d, 1H, $J = 8.4 \text{ Hz}$). ESI-MS: 334.106 $[\text{M} + \text{H}^+]$.

3-(1,3-Dioxo-1H,3H-benzo[de]isoquinolin-2-yl)-4-hydroxy-benzoic acid (**5**): Compound **5** was synthesized by the cyclo-condensation reaction of 1,8-naphthalic anhydride and 3-amino-4-hydroxy-benzoic acid with the similar procedure as used for **3**. Yield: 87%; IR (KBr, cm^{-1}): 3292 (s), 1774 (w), 1711 (s), 1698 (s), 1644 (m), 1608 (s), 1589 (m), 1510 (w), 1438 (w), 1376 (m), 1297 (m), 1270 (s), 1236 (s), 1191 (w), 1013 (w), 778 (m), 662 (w). $^1\text{H NMR}$ (400 MHz, $\text{DMSO-}d_6$): 10.61 (s, 1H), 8.49 (m, 4H), 7.89 (m, 4H), 7.07 (d, 1H, $J = 8.8 \text{ Hz}$). ESI-MS: 334.132 $[\text{M} + \text{H}^+]$.

5-hydroxy-2-[7-(2-carboxy-4-hydroxy-phenyl)-1,3,6,8-tetraoxo-3,6,7,8-tetrahydro-1H-benzo[*lmn*][3,8]phenanthroline-2-yl]-benzoic acid (**6**): A solution of 1,4,5,8-naphthalenetetracarboxylic dianhydride (1.34 g, 5 mmol) and 2-amino-5-hydroxy-benzoic acid (1.530 g, 10 mmol) in *N,N*-dimethylformamide (20 mL) was refluxed for 3 h. The reaction mixture was cooled to room temperature, poured into ice cooled water (100 mL) and stirred for 15 min. A yellow colored precipitate of the product was filtered and air-dried. Yield: 90%; IR (KBr, cm^{-1}): 3419 (m), 1736 (s), 1705 (s), 1657 (s), 1606 (m), 1583 (m), 1505 (w), 1454 (w), 1374 (m), 1361 (m), 1292 (w), 1260 (s), 1205 (s), 1154 (w), 1065 (w), 986 (w), 881 (w), 771 (m), 746 (m). $^1\text{H NMR}$ (400 MHz, $\text{DMSO-}d_6$): 10.17 (s, 2H), 8.73 (s, 4H), 7.52 (s, 2H), 7.33 (dd, 2H, $J = 8.8 \text{ Hz}$), 7.15 (d, 2H, $J = 8.4 \text{ Hz}$). ESI-MS: 584.112 $[\text{M} + \text{H}^+]$.

3-Hydroxy-2-[7-(4-carboxy-2-hydroxy-phenyl)-1,3,6,8-tetraoxo-3,6,7,8-tetrahydro-1H-benzo[*lmn*][3,8]phenanthroline-2-yl]-benzoic acid (**7**): A red colored precipitate of the product **7** was obtained by the cyclo-condensation reaction of 1,4,5,8-naphthalenetetracarboxylic dianhydride and 4-amino-3-hydroxy-benzoic acid with the similar procedure as used for **6**. Yield: 90%; IR (KBr, cm^{-1}): 3341 (m), 1712 (s), 1673 (s), 1603 (m), 1580 (m), 1426 (m), 1355 (s), 1254 (s), 1113 (w), 981 (w), 950 (w), 885 (w), 839 (m), 768 (m), 751 (m), 704 (w). $^1\text{H NMR}$ (400 MHz, $\text{DMSO-}d_6$): 10.20 (s, 2H), 8.74 (s, 4H), 7.58 (s, 2H), 7.54 (d, 2H, $J = 8.8 \text{ Hz}$), 7.46 (d, 2H, $J = 8.0 \text{ Hz}$). ESI-MS: 584.124 $[\text{M} + \text{H}^+]$.

4-Hydroxy-2-[7-(3-carboxy-6-hydroxy-phenyl)-1,3,6,8-tetraoxo-3,6,7,8-tetrahydro-1H-benzo[*lmn*][3,8]phenanthroline-2-yl]-benzoic acid (**8**): A pink colored precipitate of the product **8** was obtained by the cyclo-condensation reaction of 1,4,5,8-naphthalenetetracarboxylic dianhydride and 3-amino-4-hydroxy-benzoic acid with the similar procedure as used for **6**. Yield: 90%; IR (KBr, cm^{-1}): 3300 (m), 1707 (s), 1668 (s), 1611 (s), 1582 (m), 1514 (w), 1451 (m), 1352 (s), 1296 (m), 1260 (s), 1252 (s), 1212 (m), 1123 (w), 1087 (w), 985 (w), 841 (w), 768 (m), 648 (w). $^1\text{H NMR}$ (400 MHz, $\text{DMSO-}d_6$): 10.62 (s, 2H), 8.72 (s, 4H), 8.00 (s, 2H), 7.93 (d, 2H, $J = 8.4 \text{ Hz}$), 7.09 (d, 2H, $J = 8.8 \text{ Hz}$). ESI-MS: 584.095 $[\text{M} + \text{H}^+]$.

I: **I** was obtained by crystallization of compound **1** from pyridine solution as colorless crystals. IR (KBr, cm^{-1}): 3461 (m), 1764 (w), 1714 (s), 1631 (m), 1552 (m), 1490 (m), 1463 (m), 1391 (s), 1289 (s), 1240 (s), 1117 (m), 1087 (w), 990 (w), 887 (m), 757 (m), 718 (m), 687 (w). $^1\text{H NMR}$ (400 MHz, $\text{DMSO-}d_6$): 10.21 (s, 1H), 8.56 (d, 2H, $J = 3.6 \text{ Hz}$), 7.96 (dd, 2H, $J = 2.8 \text{ Hz}$), 7.89 (dd, 2H, $J = 2.8$

Table 1. Crystallographic Parameters of I–X

compound no.	I	II	III	IV	V
formulas	$C_{20}H_{14}N_2O_5$ ($C_{15}H_8NO_5 \cdot C_5H_6N$)	$C_{33}H_{37}N_5O_{10}$ ($C_{38}H_{21}N_2O_{10} \cdot 2C_5H_5N \cdot C_5H_6N$)	$C_{29}H_{19}N_3O_5$ ($C_{19}H_{11}NO_5 \cdot C_{10}H_8N_2$)	$C_{43}H_{37}N_5O_{14}$ ($C_{28}H_{14}N_2O_{10} \cdot 3C_5H_5N \cdot 4H_2O$)	$C_{24}H_{18}N_2O_6$ ($C_{15}H_8NO_5 \cdot C_9H_8N \cdot H_2O$)
formula wt	362.33	903.89	489.47	847.78	430.12
crystal system	triclinic	triclinic	triclinic	triclinic	triclinic
space group	$P\bar{1}$	$P\bar{1}$	$P\bar{1}$	$P\bar{1}$	$P\bar{1}$
<i>a</i> (Å)	8.0305(3)	9.3051(3)	9.5761(4)	8.4869(7)	8.1871(2)
<i>b</i> (Å)	8.0978(4)	9.3350(3)	11.3729(4)	8.8222(8)	9.4937(2)
<i>c</i> (Å)	14.9519(9)	13.7530(4)	12.5759(5)	14.4413(13)	14.0258(3)
α (°)	93.677(3)	98.580(2)	66.664(2)	105.395(6)	72.9640(10)
β (°)	91.105(3)	101.655(2)	79.047(2)	102.230(6)	80.8580(10)
γ (°)	117.764(2)	96.513(2)	66.456(2)	97.442(6)	73.4710(10)
<i>V</i> (Å ³)	857.27(7)	1144.12(6)	1152.07(8)	998.81(15)	995.86(4)
Z	2	1	2	1	2
density/Mg m ⁻³	1.404	1.309	1.411	1.403	1.397
abs coeff /mm ⁻¹	0.103	0.092	0.098	0.107	0.101
<i>F</i> (000)	376	468	508	438	435
total no. of reflections	12013	14915	12572	9249	9805
reflections, <i>I</i> > 2 σ (<i>I</i>)	2604	3233	3157	1503	2706
max (2 θ)°	50.00	50.00	50.00	41.86	50.00
ranges (<i>h</i> , <i>k</i> , <i>l</i>)	−9 ≤ <i>h</i> ≤ 9 −9 ≤ <i>k</i> ≤ 8 −17 ≤ <i>l</i> ≤ 17	−11 ≤ <i>h</i> ≤ 11 −11 ≤ <i>k</i> ≤ 11 −15 ≤ <i>l</i> ≤ 16	−11 ≤ <i>h</i> ≤ 11 −13 ≤ <i>k</i> ≤ 13 −14 ≤ <i>l</i> ≤ 14	−8 ≤ <i>h</i> ≤ 8 −8 ≤ <i>k</i> ≤ 8 −14 ≤ <i>l</i> ≤ 14	−8 ≤ <i>h</i> ≤ 9 −11 ≤ <i>k</i> ≤ 11 −16 ≤ <i>l</i> ≤ 16
complete to 2 θ (%)	97.6	99.4	97.2	99.4	91.3
data/restraints/parameters	2950/0/249	3995/0/326	3945/0/336	2114/0/310	3208/0/294
GOF (<i>F</i> ²)	1.034	1.045	1.080	1.033	1.044
<i>R</i> indices [<i>I</i> > 2 σ (<i>I</i>)]	0.0366	0.0474	0.0435	0.0564	0.0362
<i>R</i> indices (all data)	0.0408	0.0567	0.0542	0.0812	0.0432
compound no.	VI	VII	VIII	IX	X
formulas	$C_{33}H_{23}N_5O_5$ ($C_{15}H_9NO_5 \cdot 2C_9H_7N$)	$C_{83}H_{57}N_7O_{10}$ ($2C_{28}H_{18}N_2O_5 \cdot 3C_9H_7N$)	$C_{28}H_{18}N_2O_5$ ($C_{19}H_{10}NO_5 \cdot C_9H_8N$)	$C_{82}H_{56}N_8O_{10}$ ($C_{28}H_{14}N_2O_{10} \cdot 6C_9H_7N$)	$C_{91}H_{63}N_9O_{10}$ ($C_{28}H_{14}N_2O_{10} \cdot 7C_9H_7N$)
formula wt	541.54	1312.38	462.44	1313.35	1442.53
crystal system	monoclinic	monoclinic	monoclinic	triclinic	triclinic
space group	$P2_1/c$	$P2_1/c$	$P2_1/c$	$P\bar{1}$	$P\bar{1}$
<i>a</i> (Å)	12.8111(5)	9.3707(18)	9.2947(7)	9.5272(6)	7.9780(7)
<i>b</i> (Å)	28.4327(11)	19.583(4)	15.4314(12)	13.2380(9)	10.9945(9)
<i>c</i> (Å)	7.3022(3)	18.346(4)	15.7079(11)	13.3281(9)	22.1724(18)
α (°)	90.00	90.00	90.00	95.328(3)	76.991(5)
β (°)	95.295(2)	99.264(10)	95.373(4)	97.809(4)	84.185(6)
γ (°)	90.00	90.00	90.00	93.357(3)	86.845(6)
<i>V</i> (Å ³)	2648.51(18)	3322.7(12)	2243.1(3)	1653.85(19)	1884.1(3)
Z	4	2	4	1	1
density/Mg m ⁻³	1.358	1.313	1.369	1.319	1.270
abs coeff /mm ⁻¹	0.093	0.087	0.095	0.088	0.084
<i>F</i> (000)	1128	1370	960	684	751
total no. of reflections	34678	43094	29702	21948	30847
reflections, <i>I</i> > 2 σ (<i>I</i>)	3542	3883	2802	4353	3076
max (2 θ)°	50.00	47.18	50.00	50.00	50.00
ranges (<i>h</i> , <i>k</i> , <i>l</i>)	−15 ≤ <i>h</i> ≤ 14 −31 ≤ <i>k</i> ≤ 33 −8 ≤ <i>l</i> ≤ 8	−10 ≤ <i>h</i> ≤ 10 −22 ≤ <i>k</i> ≤ 21 −20 ≤ <i>l</i> ≤ 20	−11 ≤ <i>h</i> ≤ 11 −17 ≤ <i>k</i> ≤ 18 −18 ≤ <i>l</i> ≤ 18	−11 ≤ <i>h</i> ≤ 11 −15 ≤ <i>k</i> ≤ 15 −15 ≤ <i>l</i> ≤ 15	−9 ≤ <i>h</i> ≤ 9 −13 ≤ <i>k</i> ≤ 13 −25 ≤ <i>l</i> ≤ 26
complete to 2 θ (%)	99.8	98.8	100.0	99.4	98.8
data/restraints/parameters	4659/0/372	4916/0/468	3944/0/321	5810/0/453	6565/0/511
GOF (<i>F</i> ²)	1.029	1.034	1.017	1.031	1.164
<i>R</i> indices [<i>I</i> > 2 σ (<i>I</i>)]	0.0399	0.0428	0.0470	0.0421	0.0783

Table 1. continued

compound no.	I	II	III	IV	V
R indices (all data)	0.0591	0.0559	0.0698	0.0584	0.1690

Hz), 7.78 (t, 1H, $J = 7.6$ Hz), 7.43 (s, 1H), 7.38 (t, 2H, $J = 7.6$ Hz), 7.30 (d, 1H, $J = 8.8$ Hz), 7.10 (d, 1H, $J = 8.4$ Hz).

II: The crystals of **II** were obtained as colorless plates from a solution of compound **3** in pyridine. IR (KBr, cm^{-1}): 3294 (m), 1719 (s), 1694 (s), 1651 (s), 1624 (m), 1591 (m), 1500 (w), 1438 (w), 1381 (m), 1361 (m), 1292 (m), 1248 (s), 1208 (s), 1065 (w), 823 (w), 781 (m), 750 (m). $^1\text{H NMR}$ (400 MHz, $\text{DMSO}-d_6$): 10.07 (s, 1H), 8.57 (d, 3H, $J = 2.8$ Hz), 8.50 (t, 4H, $J = 7.6$ Hz), 7.90 (t, 2H, $J = 7.6$ Hz), 7.78 (t, 2H, $J = 7.2$ Hz), 7.49 (s, 1H), 7.38 (t, 3H, $J = 6.0$ Hz), 7.27 (d, 1H, $J = 8.4$ Hz), 7.11 (d, 1H, $J = 8.0$ Hz).

III: A solution of compound **4** in pyridine and a solution of bpy in ethanol were mixed together in a 1:1 ratio; red block crystals of **III** were obtained after 15 days from the solution. IR (KBr, cm^{-1}): 3444 (m), 1774 (w), 1737 (m), 1688 (s), 1650 (s), 1589 (s), 1437 (m), 1378 (m), 1357 (m), 1243 (s), 1120 (m), 1013 (m), 959 (w), 897 (w), 815 (m), 782 (m), 764 (m). $^1\text{H NMR}$ (400 MHz, $\text{DMSO}-d_6$): 10.13 (s, 1H), 8.71 (s, 4H), 8.50 (d, 4H, $J = 7.6$ Hz), 7.90 (t, 2H, $J = 7.6$ Hz), 7.80 (s, 4H), 7.56 (s, 1H), 7.50 (d, 1H, $J = 8.0$ Hz), 7.38 (d, 1H, $J = 8.4$ Hz).

IV: Compound **7** was dissolved in pyridine and left undisturbed for seven days. The crystals of **IV** were obtained as red blocks. IR (KBr, cm^{-1}): 3430 (m), 1714 (m), 1673 (s), 1582 (m), 1426 (m), 1358 (s), 1255 (s), 1214 (m), 1200 (m), 1092 (w), 981 (w), 949 (w), 883 (w), 840 (w), 768 (m), 753 (m). $^1\text{H NMR}$ (400 MHz, $\text{DMSO}-d_6$): 10.19 (s, 2H), 8.74 (s, 4H), 8.57 (s, 6H), 7.74 (t, 3H, $J = 7.2$ Hz), 7.59 (s, 2H), 7.54 (d, 2H, $J = 8.4$ Hz), 7.46 (d, 2H, $J = 8.0$ Hz), 7.37 (s, 6H).

V: **V** was crystallized as colorless blocks from the quinoline solution of compound **1**. IR (KBr, cm^{-1}): 3454 (m), 1766 (w), 1707 (s), 1593 (m), 1504 (m), 1451 (m), 1396 (s), 1290 (m), 1246 (s), 1112 (m), 1016 (w), 892 (w), 808 (w), 726 (m), 611 (w). $^1\text{H NMR}$ (400 MHz, $\text{DMSO}-d_6$): 10.20 (s, 1H), 8.90 (s, 1H), 8.36 (d, 1H, $J = 7.6$ Hz), 7.97 (m, 4H), 7.76 (t, 2H, $J = 7.2$ Hz), 7.61 (t, 1H, $J = 6.8$ Hz), 7.53 (dd, 2H, $J = 4.0$ Hz), 7.42 (s, 1H), 7.30 (d, 1H, $J = 8.4$ Hz), 7.10 (d, 1H, $J = 8.8$ Hz).

VI: The solvate **VI** was also crystallized as colorless blocks from the quinoline solution of compound **2**. IR (KBr, cm^{-1}): 3453 (m), 1780 (w), 1726 (s), 1708 (s), 1646 (m), 1596 (m), 1505 (w), 1382 (s), 1291 (m), 1228 (m), 1103 (w), 946 (w), 884 (w), 772 (m), 713 (m). $^1\text{H NMR}$ (400 MHz, $\text{DMSO}-d_6$): 10.30 (s, 1H), 8.90 (s, 2H), 8.37 (d, 2H, $J = 8.0$ Hz), 8.00 (m, 4H), 7.91 (dd, 4H, $J = 2.8$ Hz), 7.76 (t, 2H, $J = 8.0$ Hz), 7.61 (t, 2H, $J = 8.0$ Hz), 7.56 (s, 1H), 7.52 (dd, 2H, $J = 4.0$ Hz), 7.48 (d, 1H, $J = 7.6$ Hz), 7.40 (d, 1H, $J = 8.0$ Hz).

VII: The solvate **VII** was obtained from a solution of compound **3** in quinoline and pyridine after seven days as brown colored blocks. IR (KBr, cm^{-1}): 3295 (m), 1716 (s), 1693 (s), 1655 (s), 1624 (m), 1591 (m), 1582 (s), 1498 (w), 1440 (w), 1385 (m), 1296 (m), 1250 (s), 1208 (s), 1067 (w), 856 (w), 793 (m), 723 (m). $^1\text{H NMR}$ (400 MHz, $\text{DMSO}-d_6$): 10.07 (s, 1H), 8.91 (s, 2H), 8.50 (t, 4H, $J = 7.2$ Hz), 8.36 (d, 2H, $J = 8.4$ Hz), 8.01 (dd, 4H, $J = 8.4$ Hz), 7.90 (t, 2H, $J = 8.4$ Hz), 7.76 (t, 2H, $J = 6.8$ Hz), 7.61 (t, 2H, $J = 8.0$ Hz), 7.54 (dd, 2H, $J = 4.4$ Hz), 7.49 (s, 1H), 7.27 (d, 1H, $J = 8.8$ Hz), 7.11 (d, 1H, $J = 8.8$ Hz).

VIII: **VIII** was obtained by crystallization of compound **5** from quinoline solution as brown block crystals. IR (KBr, cm^{-1}): 3445 (m), 1698 (s), 1662 (s), 1589 (s), 1501 (m), 1434 (m), 1355 (s), 1291 (m), 1241 (s), 889 (w), 849 (w), 809 (m), 787 (m), 735 (w), 670 (w). $^1\text{H NMR}$ (400 MHz, $\text{DMSO}-d_6$): 10.63 (s, 1H), 8.90 (d, 2H, $J = 2.8$ Hz), 8.72 (s, 1H), 8.42 (d, 2H, $J = 7.6$ Hz), 7.88 (m, 5H), 7.76 (t, 2H, $J = 7.2$ Hz), 7.61 (t, 1H, $J = 7.6$ Hz), 7.52 (dd, 2H, $J = 4.4$ Hz), 7.10 (d, 1H, $J = 8.4$ Hz).

IX: A solution of compound **6** in pyridine and quinoline resulted in the formation of crystals of solvate **IX** as red blocks. IR (KBr, cm^{-1}): 3444 (m), 1706 (s), 1667 (s), 1530 (m), 1363 (s), 1289 (m), 1256 (s), 1222 (m), 1146 (w), 1124 (w), 771 (m). $^1\text{H NMR}$ (400 MHz, $\text{DMSO}-d_6$): 10.16 (s, 2H), 8.90 (d, 6H, $J = 2.8$ Hz), 8.71 (s, 4H), 8.36

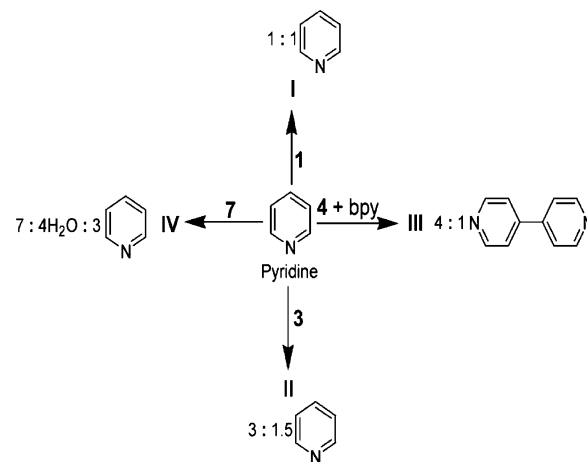
(d, 6H, $J = 8.0$ Hz), 8.00 (dd, 12H, $J = 8.4$ Hz), 7.76 (t, 6H, $J = 8.0$ Hz), 7.59 (t, 6H, $J = 8.0$ Hz), 7.33 (m, 8H), 7.32 (d, 2H, $J = 8.4$ Hz), 7.15 (d, 2H, $J = 8.8$ Hz).

X: The solvate **X** was obtained from a solution of compound **8** in quinoline and pyridine after three days as yellow blocks. IR (KBr, cm^{-1}): 3434 (m), 1712 (s), 1681 (s), 1606 (s), 1581 (s), 1504 (m), 1447 (m), 1374 (m), 1346 (s), 1301 (s), 1248 (s), 1123 (m), 1082 (m), 981 (w), 949 (w), 810 (m), 784 (m), 765 (m). $^1\text{H NMR}$ (400 MHz, $\text{DMSO}-d_6$): 10.56 (s, 2H), 8.90 (d, 7H, $J = 2.8$ Hz), 8.51 (s, 4H), 8.50 (s, 2H), 8.36 (d, 7H, $J = 7.6$ Hz), 8.00 (dd, 14H, $J = 8.0$ Hz), 7.89 (t, 7H, $J = 8.0$ Hz), 7.76 (t, 7H, $J = 7.6$ Hz), 7.61 (t, 7H, $J = 7.2$ Hz), 7.52 (dd, 2H, $J = 4.0$ Hz), 7.07 (d, 2H, $J = 8.4$ Hz).

RESULTS AND DISCUSSION

Eight different cyclic imides tethered by aromatic hydroxy carboxylic acids, **1–8**, were synthesized by condensation reactions of different cyclic anhydrides with corresponding amino hydroxy benzoic acids (Scheme 1). Crystallization of compounds **1**, **3**, and **7** with pyridine solvent led to the formation of crystals of pyridine inclusion compounds (**I**, **II**, and **IV**). The pyridine included crystals of **4** could not be obtained under the similar crystallization conditions; however, when we added 4,4'-bipyridine (bpy) in a pyridine solution of **4**, we obtained cocrystal of compound **4** with bpy in a 1:1 host–guest ratio. Host–guest ratios of all these crystalline materials are shown in Scheme 2. Different types of hydrogen

Scheme 2. Host-Guest Complexes of Imides with Pyridine/Bipyridine Showing Host-Guest Stoichiometry



bond motifs observed between the guest and multifunctional host molecules in the structures of **I–IV** are shown in Figures 1–4 along with their three-dimensional (3D) supramolecular architectures. The hydrogen bond parameters for the structures **I–IV** are listed in Table S1 (Supporting Information). Intermolecular interactions between the guest pyridine/bpy and $-\text{COOH}/-\text{OH}$ groups of host molecules lead to the formation of either salt or solvate or cocrystal. Various types of intermolecular hydrogen bonding interactions are found to be responsible for the formation of channels filled by guest molecules in all these host–guest 3D supramolecular structures.

Single crystal X-ray structure analysis reveals that compound **I** crystallized in the triclinic $P\bar{1}$ space group, and its crystallographic asymmetric unit consists of one molecule of host anion **I** and one guest pyridinium cation. In the crystal lattice of **I**, guest pyridinium molecule interacts with the carboxylate group of the host molecule via discrete donor N2–H2...O2 interaction and with the –OH group of the host molecule via discrete donor C16–H16...O3 interaction (Figure 1a). Simultaneously, another oxygen atom of carboxylate group

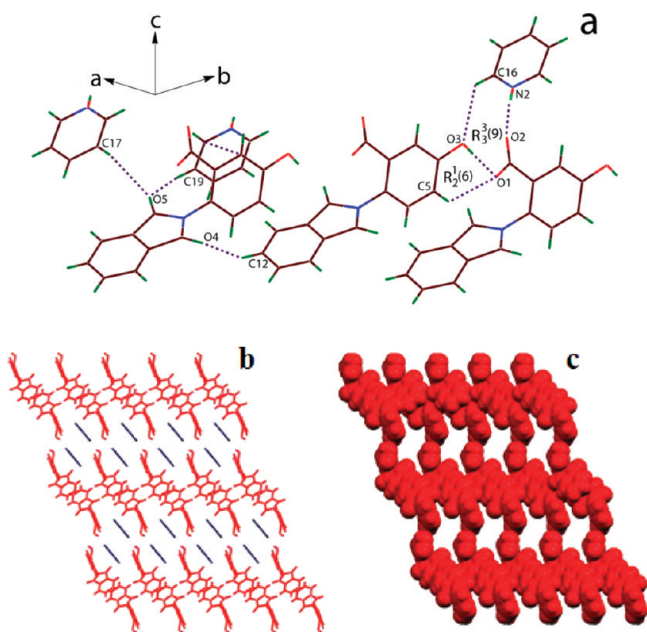


Figure 1. (a) A part of crystal structure showing host–guest weak interactions in **I**. (b) Channel formation in the assembly of host (red) and guest (blue) molecules (along the *a*-axis). (c) Space filling model after removal of pyridine molecules inside the channels.

participates in bifurcated acceptor hydrogen bonding with the –OH group and aromatic ring bearing carboxylate and –OH group of another host molecule via O3–H3A...O1 and C5–H5...O1 interactions. These interactions make an assembly of two host and one guest molecules forming two different $R_3^3(9)$ and $R_2^1(6)$ cyclic hydrogen motifs in the lattice. Further, one of the carbonyl oxygen atoms of the host molecule is also involved in bifurcated acceptor hydrogen bonding with a guest molecule via two C–H...O interactions, namely, C17–H17...O5 and C19–H19...O5 interactions. Another carbonyl oxygen interacts with the aromatic imide ring of the host molecule through C12–H12...O4 interaction. Besides that, $\pi\cdots\pi$ interactions between the aromatic rings of host and guest molecules are also observed in the hydrogen bonded assembly of **I**. All these host–guest interactions construct a 3D supramolecular layered architecture containing channels of approximate 11×6 Å dimensions in the crystal lattice of **I**. The channels formed among the two-dimensional (2D) layers of host molecules are filled by guest pyridine molecules as viewed along the *a*-axis (Figure 1b,c). These channels are constructed by tetrameric assemblies of host molecules and extend along the crystallographic *a*-axis.

The compound **II** crystallized in triclinic $P\bar{1}$ space group, asymmetric unit of this has one-half of the centrosymmetric $(3\cdots H\cdots 3)^-$ host anion with one guest pyridine molecule and half of the guest pyridinium cation. The guest pyridinium

cation, which appears as its half in the asymmetric unit, is disordered across an inversion center sharing the nitrogen and carbon atoms at the 1 and 4 positions of the pyridine ring with half occupancies. The hydrogen atom attached to the carboxylate group of host molecule is also disordered and shared between the two same oxygen atoms of two carboxylate groups by O2–H2...O2 interaction (Figure 2a). The hydrogen

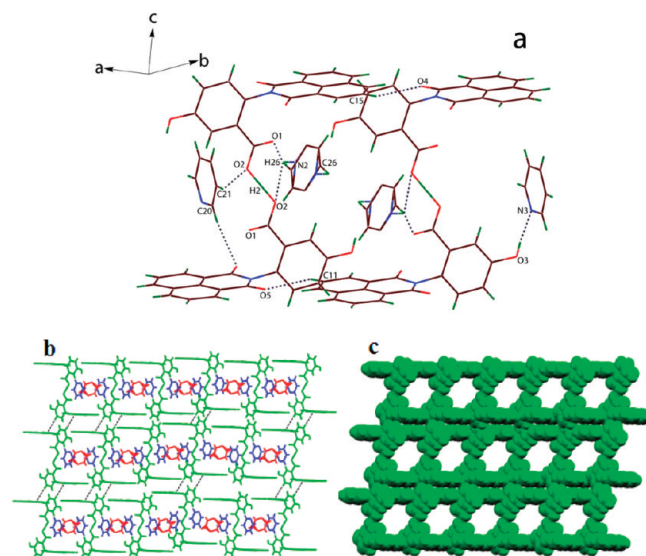


Figure 2. (a) Weak interactions in the host–guest assembly of **II**. (b) Formation of 3D channel architecture where 2D separated layers of host molecules (green) are sustained by C–H... π interactions containing pyridinium cations and pyridine molecules (red and blue) inside the channels (along the *a*-axis). (c) Space filling model after removal of guest molecules inside the channels.

atom located on disordered pyridinium cation is also shared with this oxygen atom by N2–H26...O2 interaction which also participates in bifurcated donor hydrogen bonding and further interacts with another oxygen atom of the carboxylate group by N2–H26...O1 interaction. The guest pyridine molecule also interacts with the carboxylate group, –OH group, and carbonyl oxygen atom of the host molecule by donor–acceptor C21–H21...O2, O3–H3A...N3, and C20–H20...O4 interactions, respectively. The host molecules also assemble in the lattice by C11–H11...O5 and C15–H15...O4 interactions which exist between the carbonyl oxygen atoms and naphthalimide rings. These interactions result in the construction of 2D layers of host molecules containing channels of approximate 11×9 Å dimensions in the lattice. The 2D layers are further connected to each other via C–H... π ($d_{C5\cdots\pi}$ 3.54 Å) interactions creating a 3D host–guest architecture of **II** in the crystal lattice (Figure 2b). The channels formed inside the 2D layers of the host molecules are filled by both guest pyridinium cations and pyridine molecules as viewed along the *a*-axis (Figure 2b,c). Earlier in the case of pyridine solvates of various naphthalimide tethered carboxylic acids, we have demonstrated that the guest molecule interacts with the host molecule either making a cyclic $R_2^2(7)$ hydrogen bond motif or via a discrete O–H...N interaction.^{11a}

The cocrystal **III** crystallized in the triclinic $P\bar{1}$ space group and possesses one molecule of host **I** and one molecule of guest bpy in its crystallographic asymmetric unit. In the structure of **III**, the guest bpy molecule loses its planarity, and both the aromatic rings are twisted at an angle of 32° with

respect to each other. The guest bpy molecule is found to associate with host molecules via both donor and acceptor host–guest interactions (Figure 3a). Both the nitrogen atoms

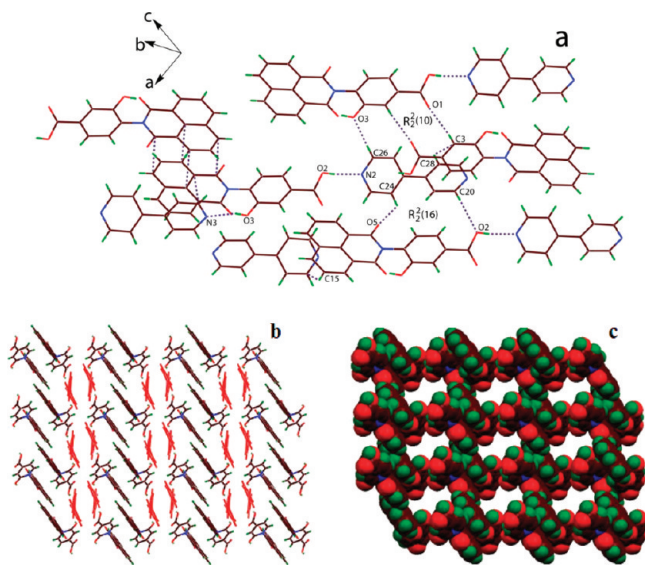


Figure 3. (a) Weak interactions among the host and guest bpy molecules in **III**. (b) Crystal packing arrangement showing 3D channels along the *b*-axis. (c) Space filling model after omission of guest bpy (red) molecules inside the channels.

of bpy interact with $-\text{COOH}$ and $-\text{OH}$ functional groups of host molecule via acceptor $\text{O2}-\text{H2}\cdots\text{N2}$ and $\text{O3}-\text{H3}\cdots\text{N3}$ interactions and its aromatic ring also interacts with the naphthalimide ring of the host molecule via acceptor $\text{C}-\text{H}\cdots\pi$ ($d_{\text{C15}\cdots\pi}$ 3.57 Å) interaction. The aromatic rings of guest bpy molecule are also found to display four different donor hydrogen bonds with host molecule, namely, $\text{C20}-\text{H20}\cdots\text{O2}$ and $\text{C24}-\text{H24}\cdots\text{O5}$ interactions with $-\text{COOH}$ group and carbonyl oxygen making a cyclic $\text{R}_2^2(16)$ hydrogen bond motif, another $\text{C26}-\text{H26}\cdots\text{O3}$ interaction with the $-\text{OH}$ group, and $\text{C28}-\text{H28}\cdots\pi$ ($d_{\text{C28}\cdots\pi}$ 3.50 Å) interaction with the aromatic ring of the host molecule. Moreover, the $\pi\cdots\pi$ interactions between the naphthalimide ring of the host molecule and one of the aromatic rings of the guest molecule are also observed in the lattice. No interactions between the guest molecules are observed; however, the host molecules are found to interact with each other by a combination of two similar $\text{C3}-\text{H3A}\cdots\text{O1}$ interactions between the oxygen atom of the $-\text{COOH}$ groups and the hydrogen atom of the aromatic ring, forming a cyclic $\text{R}_2^2(10)$ motif in the lattice. Strong $\pi\cdots\pi$ contact between the naphthalimide rings of host molecules are also observed in the hydrogen bonded network of **III**. All the intermolecular host–host and host–guest hydrogen bond interactions can be taken in account for the construction of a 3D supramolecular channel network of **III** in the crystal lattice. The channels of approximate 16×10 Å dimensions are created by repeated 3D hexameric assemblies of host molecules. The guest molecules are encapsulated inside these assemblies filling the channels as viewed along the *b*-axis (Figure 3b,c). Bipyridine or terpyridines have been used to make porous building blocks with aromatic carboxylic acids.¹⁴

The solvate **IV** crystallized in the triclinic $\bar{P}1$ space group and included a half molecule of **7** lying on the inversion center, one and half molecules of guest pyridine, and two molecules of

solvent water in its crystallographic asymmetric unit. The guest pyridine molecule, which appears as its half in the asymmetric unit, is disordered across an inversion center and disposed in the lattice such that the nitrogen and carbon atoms at 1 and 4 positions of the pyridine rings are shared with half occupancies (Figure 4a). This symmetric arrangement produces two sets of

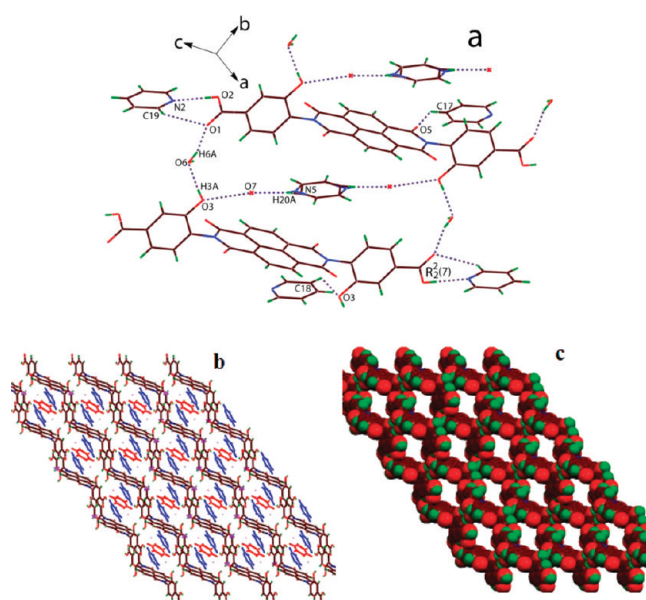


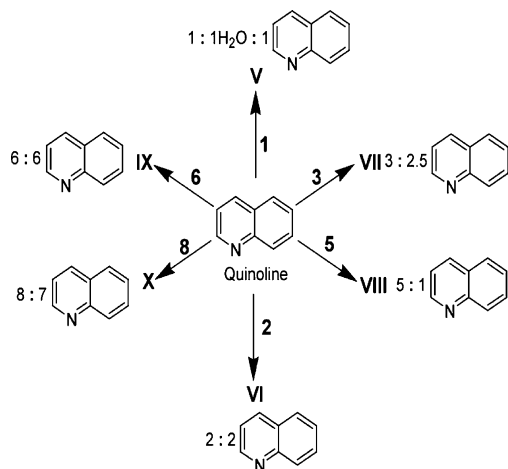
Figure 4. (a) Host–guest weak interactions forming a 1D supramolecular cavity in the structure of **IV**. (b) Formation of 3D channels (along the *c*-axis) containing guest pyridine and water molecules inside the channels in the supramolecular architecture of **IV**. (c) Space filling model after removal of guest molecules inside the channels.

symmetry nonequivalent guest pyridine (total three) and two sets of symmetry independent water molecules (total four) in the lattice. One set of lattice water molecules interacts with the $-\text{COOH}$ and $-\text{OH}$ groups of the host molecule via donor–acceptor $\text{O6}-\text{H6A}\cdots\text{O1}$ and $\text{O3}-\text{H3A}\cdots\text{O6}$ interactions and assemble two host and two lattice water molecules in a 1D layered arrangement forming repeated supramolecular cavities in the lattice. The cavities that formed along the *a*-axis contain disorder pyridine (from one set) and another set of water molecules interacting with each other via $\text{N5}-\text{H20A}\cdots\text{O7}$ interactions. No interactions between the host molecules or same guest molecules are observed in the crystal lattice of **IV**. Another set of guest pyridine molecules are associated with the $-\text{COOH}$ group of host molecules by a combination of donor–acceptor $\text{C19}-\text{H19}\cdots\text{O1}$ and $\text{O2}-\text{H2}\cdots\text{N2}$ interactions making cyclic $\text{R}_2^2(7)$ hydrogen bond motifs and further interacts with the $-\text{OH}$ and carbonyl group of host molecules through donor $\text{C18}-\text{H18}\cdots\text{O3}$ and $\text{C17}-\text{H17}\cdots\text{O5}$ interactions. These interactions assemble the one-dimensional (1D) layers into a 3D supramolecular host–guest network. The 3D network created by host–guest interactions also form channels of approximate 16×6 Å dimensions in the lattice along the *c*-axis. These channels created between the 3D layers of host molecules are filled by both sets of guest water and pyridine molecules (Figure 4b,c). We have also shown earlier that different orientations of the weak interactions lead to polymorphic structures in pyridine solvates of naphthalene diimide tethered carboxylic acids.^{11b}

Powder X-ray diffraction (PXRD) patterns of all these host–guest crystalline materials are recorded, which are almost the same as that simulated patterns from the single-crystal data, revealing the phase purity of the bulk samples (Figures S1–S4, Supporting Information). To examine the host–guest ratios in the pyridine inclusion compounds, thermogravimetric analyses (TGA) are carried out (Figures S11–S13, Supporting Information). TGA curve of **I** shows one-step weight loss of 20.7% weight in the temperature range 95–150 °C corresponds to one equivalent of pyridine molecule (calcd 21.8%). Compound **II** loses 27.6% weight in two steps between 85 and 140 °C, which corresponds to the loss of one and half equivalent of pyridine molecules (calcd 26.3%). In solvate **IV**, the weight loss between 25 and 55 °C is accounted for by the loss of lattice water molecules; a further 29.4% weight loss corresponds to three equivalents of pyridine molecules, occurring from **IV** in the temperature range 90–160 °C (calcd 30.5%).

Crystal structures of six quinoline inclusion compounds (**V**–**X**) of different cyclic imides were also determined. The host–guest stoichiometries of these compounds are depicted in Scheme 3. The guest quinoline molecules are found to associate

Scheme 3. Various Inclusion Compounds of Quinoline Showing Host–Guest Ratio



with host molecules via different types of weak interactions in the structures of **V**–**X** (Figures 5–10). The supramolecular architectures of these various structures create different types of channels in their crystal lattices which are filled by guest molecules. The hydrogen bond parameters for the structures **V**–**X** are listed in Table S2 in Supporting Information.

Crystal structure analysis revealed that compound **V** crystallized in the triclinic $P\bar{1}$ space group, and its crystallographic asymmetric unit contains one molecule of host anion **1**, one guest quinolinium cation, and one lattice water molecule. In the crystal lattice of **V**, the host molecules associate with each other through a set of two O3–H3A...O2 interactions between the carboxylate and –OH functional groups which produce $R_2^2(14)$ motifs in the lattice (Figure 5a). One of the carbonyl oxygen atoms of host molecules interacts with aromatic imide rings via C11–H11...O5 interactions. This arrangement of weak interactions leads to the formation of 1D cavities along the *a*-axis involving four host molecules in such a cavity. The guest water and quinolinium molecules are held in these cavities by weak interactions. The oxygen atoms of water

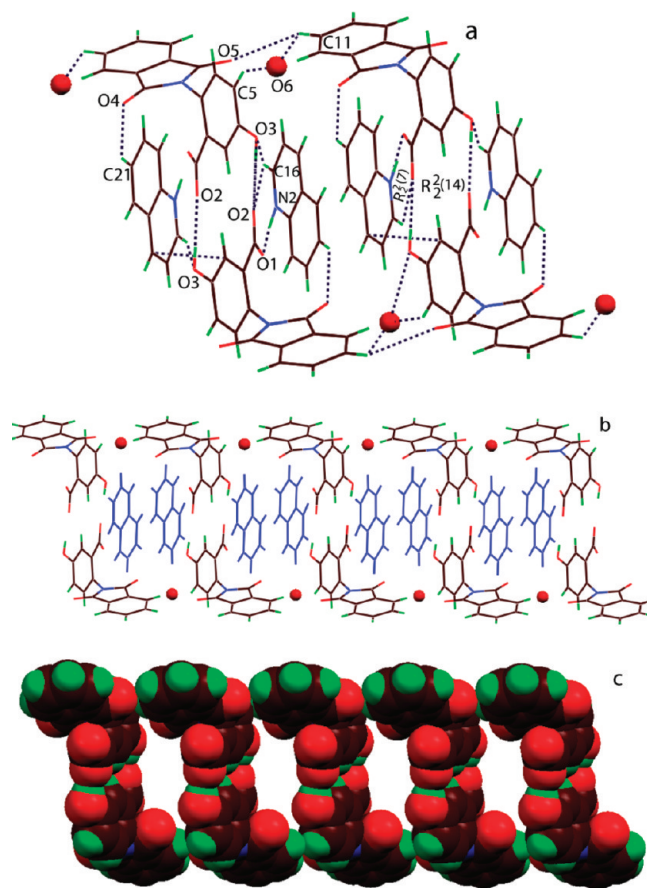


Figure 5. (a) Host–guest interactions leading to the formation of a cavity containing guest molecules (along the *a*-axis) in the structure of **V**. (b) Construction of a 2D host–guest channel network in the lattice (along the *b*-axis). (c) Space filling model after removal of guest quinolinium (blue) and water (red) molecules inside the channels.

molecules form bifurcated hydrogen bonds with the aromatic rings of host molecules via C5–H5...O6 and C11–H11...O6 interactions. The guest quinolinium molecules interact with the carboxylate groups of host molecules to make $R_2^2(7)$ motifs via N2–H2...O1 and C16–H16...O2 interactions and also come in contact with –OH groups via weak C16–H16...O3 hydrogen bonds inside these cavities. The quinolinium molecules further interact with host molecules through C21–H21...O4 and $\pi\cdots\pi$ interactions, constructing a 2D channel architecture of host molecules in the lattice. These 2D channels of approximate 11 × 10 Å dimensions are occupied by guest molecules as viewed along the *b*-axis (Figure 5b,c).

The solvate **VI** crystallized in monoclinic $P2_1/c$ space group and involves one molecule of host **2** and two symmetry nonequivalent guest quinoline molecules in the crystallographic asymmetric unit. One of the symmetry nonequivalent quinoline molecules interacts with the –COOH of group host molecule via discrete O2–H2...N2 interaction (Figure 6a). The hydrogen atom of this quinoline ring also forms a bifurcated donor hydrogen bond with the carbonyl oxygen atom and aromatic ring of host molecule via C17–H17...O4 and C–H... π ($d_{C17\cdots\pi}$ 3.65 Å) interactions. Another symmetry nonequivalent quinoline molecule is found to associate with –OH and carbonyl groups of host molecule by a combination of acceptor O3–H3A...N3 and donor C25–H25...O5 interactions making a cyclic $R_2^2(10)$ motif in the lattice. This quinoline also interacts

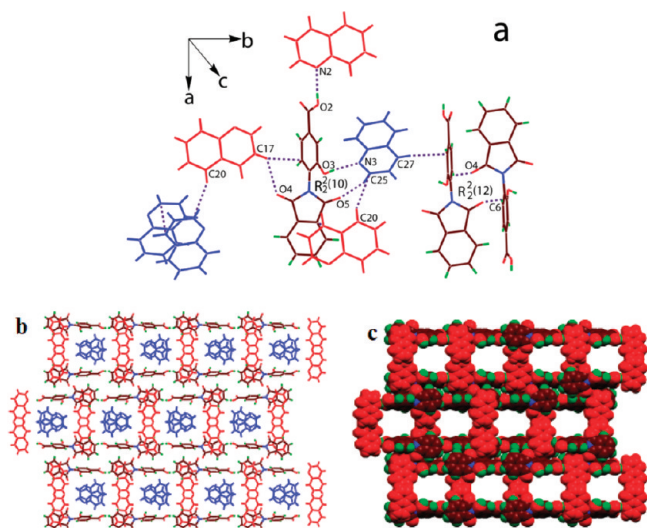


Figure 6. (a) Intermolecular interactions between the host and two symmetry independent guest molecules in VI. (b) Formation of 3D supramolecular channel architecture by the combination of host molecules and one set of symmetry independent guest molecules (along the *c*-axis). (c) Space filling model after removal of another set of guest quinoline molecules inside the channels.

with the aromatic ring of the host molecule bearing $-\text{COOH}$ and $-\text{OH}$ groups via $\text{C}-\text{H}\cdots\pi$ ($d_{\text{C}27\cdots\pi}$ 3.61 Å) interaction. Moreover, $\text{C}-\text{H}\cdots\pi$ ($d_{\text{C}20\cdots\pi}$ 3.69 Å) interactions between the two different sets of symmetry nonequivalent guest molecules and $\pi\cdots\pi$ interactions between the same set of guest molecules are also observed in the lattice. Beside that, the host molecules also assemble together to create a cyclic $\text{R}_2^2(12)$ motif in the lattice via edge to face $\text{C}6-\text{H}6\cdots\text{O}4$ interactions. All the above-described host–host, host–guest, and guest–guest interactions affect the construction of a 3D supramolecular structure creating channels of approximate 11×9 Å dimensions in the crystal lattice of VI. These channels are constructed by the combination of host and one set of symmetry independent guest molecules in the separated 2D host–guest layers and accommodate another independent set of guest molecules inside them as viewed along the *c*-axis (Figure 6b,c).

The solvate VII crystallized in the monoclinic $P2_1/c$ space group; its crystallographic asymmetric unit consists of one molecule of host 3 and two and half guest quinoline molecules. The guest quinoline molecule, which appears as its half in the asymmetric unit, is disordered and maintains a symmetric structure with respect to an inversion center. The disordered structure is formed by sharing two nitrogen atoms with half occupancies with two carbon atoms at two opposite sites. This arrangement makes three symmetry nonequivalent quinoline molecules in the asymmetric unit which interact with the host molecule via different types of interactions (Figure 7a). The hydrogen atom attached to the $-\text{COOH}$ group of the host molecule is also disordered and shared with one set of symmetry independent (first set) guest quinoline molecules via $\text{O}1-\text{H}1\cdots\text{N}2$ interaction. The first set of quinoline molecules further interacts with another oxygen atom of the $-\text{COOH}$ group and oxygen atom of the $-\text{OH}$ group via donor $\text{C}20-\text{H}20\cdots\text{O}2$ and $\text{C}26-\text{H}26\cdots\text{O}3$ interactions and also shows a bifurcated donor $\text{C}-\text{H}\cdots\pi$ ($d_{\text{C}22\cdots\pi}$ 3.73 Å and 3.67 Å) interaction with the naphthalimide ring of the host molecule. The second set of quinoline molecule interacts with the $-\text{OH}$ group of the host molecule via acceptor $\text{O}3-\text{H}3\text{A}\cdots\text{N}3$

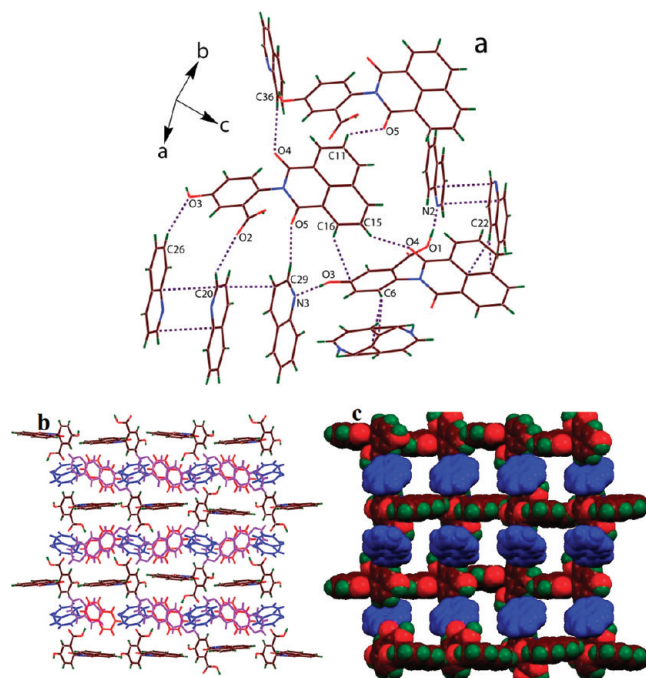


Figure 7. (a) A part of the crystal structure of VII showing different types of weak interactions between the host and three symmetry independent quinoline molecules. (b) Channel formation in the assembly of host and quinoline molecules (along the *c*-axis). (c) Space filling model after removal of first and second set of quinoline molecules inside the channels.

interaction and with both the carbonyl oxygen atoms of the host molecule via donor $\text{C}29-\text{H}29\cdots\text{O}5$ and $\text{C}36-\text{H}36\cdots\text{O}9$ interactions. The disorder quinoline molecule (third set) interacts with the host molecule via bifurcated acceptor $\text{C}-\text{H}\cdots\pi$ ($d_{\text{C}22\cdots\pi}$ 3.65 Å and 3.49 Å) interactions. Beside these host–guest interactions, the host molecules also interact with each other in the lattice via $\text{C}11-\text{H}11\cdots\text{O}5$ and $\text{C}15-\text{H}15\cdots\text{O}4$ and $\text{C}-\text{H}\cdots\pi$ ($d_{\text{C}16\cdots\pi}$ 3.62 Å) interactions. Strong $\pi\cdots\pi$ interaction between the first set of quinoline molecules and between the first and second set of quinoline molecules are also observed in the crystal lattice. These interactions give rise to a 3D supramolecular host–guest assembly creating channels of approximate 10×5 Å dimensions in the lattice as viewed along the *c*-axis. The channels are formed by the combinations of host and disordered quinoline molecules, containing other two sets of quinoline molecules inside these channels (Figure 7b,c).

The compound VIII crystallized in the monoclinic $P2_1/c$ space group, containing one molecule of host anion 5 and one guest quinolinium cation in its crystallographic asymmetric unit. The hydrogen atom attached with a guest quinolinium molecule acts as a disordered hydrogen in the structure of VIII and is shared with the carboxylate group of the host molecule via $\text{N}2-\text{H}2\cdots\text{O}2$ interaction (Figure 8a). Another oxygen atom of the carboxylate group of the host molecule forms a intermolecular bifurcated acceptor hydrogen bond with the aromatic ring of another host molecule by the combination of $\text{O}3-\text{H}3\text{A}\cdots\text{O}2$ and $\text{C}4-\text{H}4\cdots\text{O}1$ interactions generating a $\text{R}_2^1(6)$ motif in the lattice. Carbonyl groups and naphthalimide rings of the host molecules also interact with each other via $\text{C}15-\text{H}15\cdots\text{O}4$ interactions and create a 2D arrangement of host–guest molecules. Further to this, aromatic rings of guest quinolinium molecules interact with the oxygen atoms of the

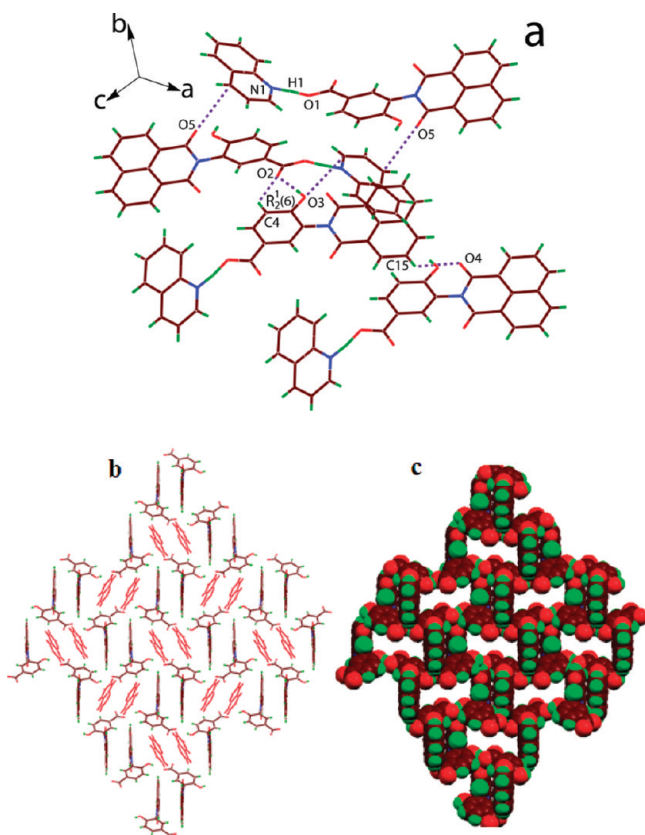


Figure 8. (a) Intermolecular interactions in a part of crystal structure of VIII. (b) 3D hexameric assemblies of host molecules creating channels along the *a*-axis. (c) Space filling model after removal of guest molecules inside the channels.

–OH group and carbonyl group of host molecules via $O \cdots \pi$ ($d_{O3 \cdots \pi}$ 3.21 Å and $d_{O5 \cdots \pi}$ 3.21 Å) interactions. Consequently, individual 2D layers pack together to construct a 3D supramolecular host–guest channel network in the lattice where repeated hexameric assemblies of host molecules are involved in the formation of an individual channel of approximate 14×5 Å dimension. The channels formed by repeated 3D hexameric assemblies of host molecules accommodate the guest quinoline molecules as viewed along the *a*-axis (Figure 8b,c).

The solvate IX crystallized in the triclinic $P\bar{1}$ space group and it contains a half molecule of 6 lying on the inversion center with three symmetry nonequivalent guest quinoline molecules in its crystallographic asymmetric unit. In the crystal lattice of IX, all the three symmetry independent quinoline molecules are found to associate with the host molecule via different weak interactions (Figure 9a). First set of quinoline molecules form a cyclic $R_2^1(6)$ hydrogen bond motif interacting with the –OH and aromatic ring of the host molecule by the combination of acceptor $O3-H3A \cdots N2$ and $C3-H3 \cdots N2$ interactions. This quinoline molecule also demonstrates some other weak interactions, namely, donor $C16-H16 \cdots O5$ and acceptor $C3-H3A \cdots \pi$ ($d_{C3 \cdots \pi}$ 3.69 Å) interactions with the carbonyl group and aromatic ring of the host molecule, respectively. Another set of quinoline molecules participate in the formation of a discrete $O2-H2 \cdots N3$ hydrogen bond with the –COOH group of the host molecule. A third set of quinoline molecules does not facilitate by $O-H \cdots N$ interactions but interacts with the oxygen atoms of the –COOH and carbonyl groups of the

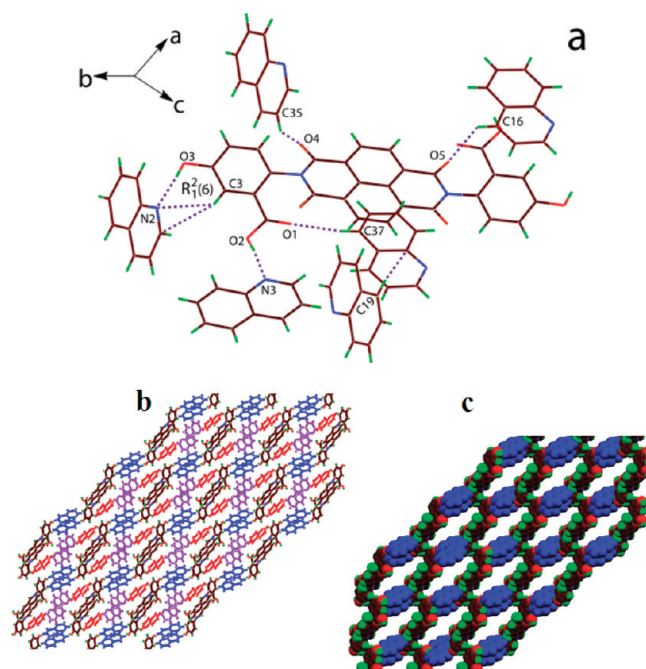


Figure 9. (a) Host–guest interactions in a part of the crystal structure of IX. (b) 3D supramolecular architecture containing two different sets of guest molecules inside the channels (along the *a*-axis). (c) Space filling model after removal of guest quinoline (blue and red) molecules inside the channels.

host molecule via discrete donor $C37-H37 \cdots O1$ and $C35-H35 \cdots O4$ interactions, respectively. The host molecules do not enclose any weak interaction between them. The guest quinoline molecules belonging to the first and third set interact with each other only via $C-H \cdots \pi$ ($d_{C19 \cdots \pi}$ 3.75 Å) interaction. The $C-H \cdots O$ interactions between the host molecules and first set of quinoline molecules aggregate them in a 1D layer. Further, creation of a 3D channel-like supramolecular structure occurs in the lattice by the other interactions experienced between host and quinoline molecules. The second and third set of quinoline molecules do not participate in the channel formation. However, the channels (approximate 20×11 Å dimensions) created by the combination of the first set of quinoline and host molecules accommodate the second and third set of quinoline molecules as viewed along the *a*-axis (Figure 9b,c). A quinoline solvate of dopamine based pyromellitic diimide host is reported to create channels in the lattice in which two sets of symmetry nonequivalent guest molecules are found to be involved in the construction of channels, whereas the third set of guest molecules takes position inside the channels.^{11c}

The solvate X crystallized in the triclinic $P\bar{1}$ space group and it contains a half molecule of 8 lying on the inversion center with three and half symmetry nonequivalent guest quinoline molecules in the crystallographic asymmetric unit. The guest quinoline molecule, which appears as its half in the asymmetric unit, is disordered the same as in the case of structure VII. In the crystal lattice of X, the host molecules do not interact with each other in any kind of weak interaction (Figure 10a). Likely, no interaction between the disorder quinoline and host molecule is observed in the lattice. The remaining three symmetry independent quinoline molecules have different types of interactions with the host molecule. The first set of quinoline molecules has three different types of interactions

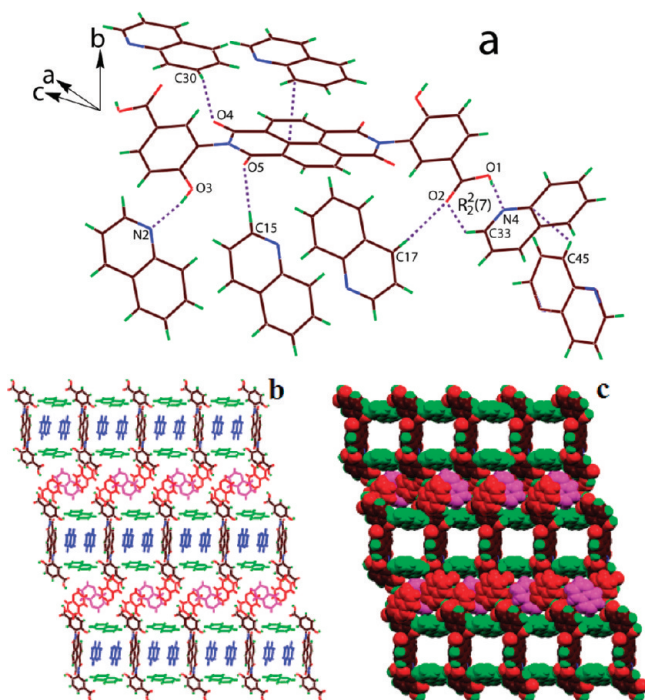


Figure 10. (a) Host-guest interactions in a part of the crystal structure of X. (b) 3D host-guest channels architecture containing a set of guest molecules inside the channels. (c) Space filling model after the removal of guest quinoline molecules inside the channels.

with the host molecule: two donor C17-H17...O2 and C15-H15...O5 interactions with the -COOH and carbonyl groups,

respectively, and one acceptor O3-H3A...N2 interaction with the -OH group. The second set of quinoline molecule forms a cyclic R₂²(7) hydrogen bond motif with the -COOH group by the combination of donor-acceptor O1-H1...N4 and C33-H33...O2 interaction. The third set of quinoline molecules interacts with the carbonyl group of the host molecule via the donor C30-H30...O4 interaction, simultaneously showing strong $\pi\cdots\pi$ contacts with the naphthalene ring of the host molecule. These host-guest interactions are found to be responsible for the formation of a 2D layered network of host and guest molecules in the lattice. These 2D layers are further grown along the *a*-axis via guest-guest C-H... π ($d_{C45\cdots\pi}$ 3.44 Å) interactions experienced between the disordered and second set of quinoline molecules. Thus, a 3D supramolecular host-guest architecture is constructed in the lattice which contains 2D rectangular channels of approximate 11 × 11 Å dimension along the *a*-axis. The channels are formed by the layered arrangement of the host and first set of quinoline molecules. A third set of quinoline molecules are sandwiched inside these channels via weak interactions. The disordered and second set of guest molecules do not take part in the formation of channels but participate in the enhancement of supramolecular architecture from 2D to 3D through weak interactions in the crystal lattice (Figure 10b,c). However, the quinoline solvates of naphthalene diimide tethered carboxylic acids have been reported to form pseudopolymorphic structures via different types of host-guest interactions, but the formation of channels in these structures may be attributed to the role of additional O-H...N interactions that exist between the -OH group of the host molecule and guest quinoline molecules.

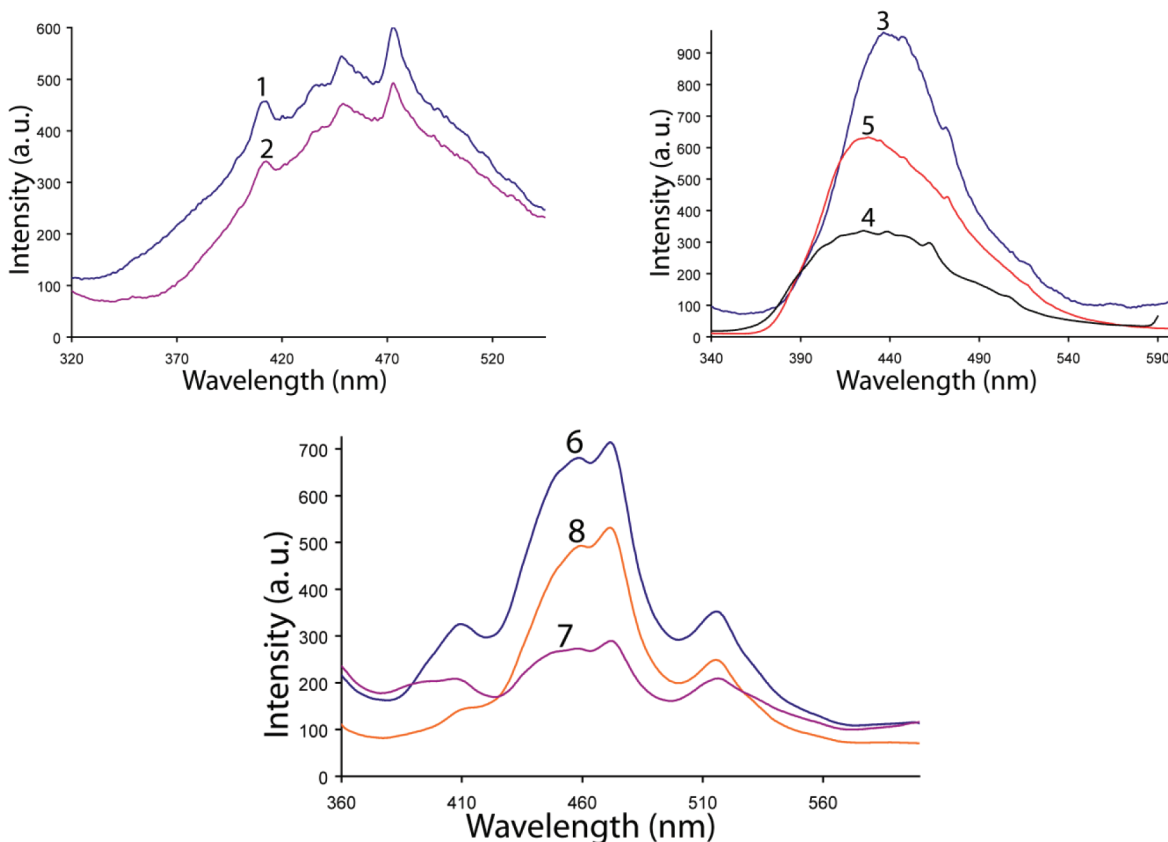


Figure 11. Solid state fluorescence emission spectra of host compounds, 1-8.

The PXRD patterns of all the quinoline solvates are shown in Figures S5–S10 in the Supporting Information. All of the peaks of different solvates can be correlated nearly with their respective simulated PXRD patterns of single crystal X-ray structures. However, some small deviations are attributed to the loss of solvent molecules leading to loss of crystallinity. TGA on quinoline solvates was also carried out (Figures S14–S19). TGA curve of **V** reveals the loss of 32.7% weight corresponding to one equivalent of water and one equivalent of quinoline molecule in the temperature range 125–220 °C (calcd 34.1%). In solvate **VI**, 47.9% weight loss occurs in one step between 100 and 185 °C, which corresponds to two equivalents of quinoline molecules (calcd 47.7%). Solvate **VII** loses two and half equivalents of quinoline molecules in two steps between 95 and 210 °C; in the first step, 29.1% weight loss occurs between 95 and 155 °C, which is accounted for by the loss of one and half quinoline molecules (calcd 29.5%). Further, a 27.7% weight loss for one quinoline molecule occurs in the second step in the temperature range 160–210 °C. Compound **VIII** shows one step weight loss of 28.1% weight between 145 and 185 °C corresponding to one equivalent of quinoline molecule (calcd 27.9%). Weight loss of six guest quinoline molecules occurs in two steps from **IX**. In the first step, a 39.0% weight loss corresponds to four equivalent of quinoline molecules, which occurs between 115 and 150 °C (calcd 39.3%). In the second step, a 31.9% weight loss occurs from the residue of the first step for remaining two guest quinoline molecules between 210 and 245 °C (calcd 32.4%). For the solvate **X**, a continuous weight loss due to the seven equivalents of quinoline molecules takes place in the temperature range 115–275 °C corresponding to a weight loss of 58.7% (calcd 62.6%).

Fluorescence Emission of Compounds. The fluorescence emission properties of analogous naphthalimide compounds have been reported.^{7a,15} These compounds are also no exception to that and they show emissions in the blue spectral region in both solution and solid state studies. So, it prompted us to investigate the fluorescence properties of our compounds in view of potential applications as fluorescent brighteners.¹⁶

The solid state fluorescence emission spectra of host compounds **1–8** are shown in Figure 11. Upon excitation at 300 nm, three emission peaks at 412 nm, 450 and 473 nm are observed for phthalimide derivatives **1** and **2**. For naphthalimide derivatives **3**, **4**, and **5**, the excitation wavelength (λ_{ex}) was at 320 nm. These compounds show strong emission bands in the 428–440 nm region. The emission spectra of naphthalene diimide derivatives **6**, **7**, and **8** are recorded at λ_{ex} 340 nm, which show strong peaks at 472 nm along with two shoulder peaks at 458 and 516 nm, respectively. However, it is observed that relative intensities of the emission peaks of isomeric hosts are also different from each other, which is probably due to the differences in the supramolecular structures of the compounds that contained similar functional groups at different positions of the aromatic rings.¹⁷ The emission spectra of pyridine and quinoline inclusion compounds **I–X** are also recorded, but no significant differences are detected in the emission peaks of hosts and their respective inclusion compounds except the intensities of emission peaks; therefore, those are not included in this study.

CONCLUSIONS

Structural features of host–guest complexes of pyridine and quinoline with a series of hydroxy benzoic acids that are tethered by phthalimide, naphthalimide, or naphthalene diimide

units are studied. This study illustrates the role of supra-molecular interactions between two different functional groups and pyridine/quinoline along with the combined effects of π -stacking aromatic imide synthons to provide the directional properties to these host–guest systems. It is also clear from this study that stability of the channels, which are filled by guest molecules, are guided by various types of intermolecular host–guest interactions. We could distinguish two different classes of channels; namely, one is those constructed by the self-assembly of hosts containing the guest molecules within them. Another category includes the channels formed by the combination of both host and guest molecules containing additional guest molecules inside them. Since the guest molecules studied here are relatively bigger in size than conventional solvent molecules, we identified the symmetry associated with the guest molecules and found that there are symmetry nonequivalent guests in certain cases; for example, a system which embedded six molecules of quinoline, namely, **IX**, has two symmetry nonequivalent guest molecules within the channel. This happens by different orientations of the host–guest interactions in the channel to make them symmetry independent. We observed that apart from hydrogen bond interactions between the host and guest molecules, some other host–host or host–guest interactions (such as π – π and C–H \cdots π) led to the inclusion of different numbers of guest molecules with isomeric host molecules; for example, in the case of quinoline inclusion compounds, the structures of **V** and **VI** are composed of one and two guest molecules, respectively, containing isomeric phthalimide host molecules. The structures of **VII** and **VIII** are composed of five per two and one guest molecule, respectively, containing isomeric naphthalimide host molecules; similarly, structures of **IX** and **X** are composed of six and seven guest quinoline molecules, respectively, containing isomeric naphthalene diimide host molecules. The structures of **IX** and **X** contain a higher number of guest molecules and serve as excellent storage systems for quinoline molecules by organic hosts.

ASSOCIATED CONTENT

Supporting Information

CIF files, simulated and experimental PXRD patterns, and TGA curves are available. This material is available free of charge via the Internet at <http://pubs.acs.org>.

AUTHOR INFORMATION

Corresponding Author

*E-mail: juba@iitg.ernet.in. Phone: + 91-361-2582311. Fax: + 91-361-2690762.

Notes

The authors declare no competing financial interest.

ACKNOWLEDGMENTS

The authors thank Department of Science and Technology, New Delhi (India) for financial support. One of the authors (D.S.) is thankful to Council of Scientific and Industrial Research, New Delhi (India) for a senior research fellowship.

REFERENCES

- (1) (a) Yang, W.; Greenaway, A.; Lin, X.; Matsuda, R.; Blake, A. J.; Wilson, C.; Lewis, W.; Hubberstey, P.; Kitagawa, S.; Champness, N. R.; Schroder, M. *J. Am. Chem. Soc.* **2010**, *132*, 14457. (b) Gonzalez-Rodriguez, D.; Schenning, A. P. H. *J. Chem. Mater.* **2011**, *23*, 310. (c) Russell, V. A.; Evans, C. C.; Li, W.; Ward, M. D. *Science* **1997**, *276*,

575. (d) Klaus, M.; Vasylyeva, V. *CrystEngComm* **2010**, *12*, 3989. (e) Anthonya, S. P.; Varughesea, S.; Drapera, S. M. *J. Phys. Org. Chem.* **2010**, *23*, 1074. (f) Amabilino, D. B.; Veciana, J. *Top. Curr. Chem.* **2006**, *265*, 253. (g) Desiraju, G. R. *Chem. Commun.* **1997**, 1475. (h) Reddy, D. S.; Craig, D. C.; Desiraju, G. R. *J. Am. Chem. Soc.* **1996**, *118*, 4090. (i) Desiraju, G. R. *Angew. Chem., Int. Ed.* **1995**, *34*, 2311. (j) Varshney, D. B.; Papaefstathiou, G. S.; MacGillivray, L. R. *Chem. Commun.* **2002**, 1964. (k) Etter, M. C. *Acc. Chem. Res.* **1990**, *23*, 120.
- (2) (a) Horneffer, V.; Dreisewerd, K.; Ludemann, H. C.; Hillenkamp, F.; Lage, M.; Strupat, K. *Int. J. Mass Spectrom. Ion Process* **1999**, *185*, 859. (b) Agmon, L.; Herbststein, F. H. *Eur. Cryst. Meet.* **1982**, *7*, 50. (c) Mazurek, J.; Dova, E.; Helmond, R. *Acta Crystallogr.* **2007**, *E63*, o3289. (d) Gdaniec, M.; Gilski, M.; Denisov, G. S. *Acta Crystallogr.* **1994**, *CS0*, 1622. (e) Luo, T. J. M.; Palmore, G. T. R. *Cryst. Growth Des.* **2002**, *2*, 337. (f) Sarma, B.; Roy, S.; Nangia, A. *Chem. Commun.* **2006**, 4918. (g) Roy, S.; Bhatt, P. M.; Nangia, A.; Kruger, G. J. *Cryst. Growth Des.* **2007**, *7*, 476. (h) McGrady, G. S.; Odlyha, M.; Prince, P. D.; Steed, J. W. *CrystEngComm* **2002**, *4*, 271.
- (3) (a) Sarma, B.; Sanphui, P.; Nangia, A. *Cryst. Growth Des.* **2010**, *10*, 2388. (b) Sarma, B.; Nath, N. K.; Bhogala, B. R.; Nangia, A. *Cryst. Growth Des.* **2009**, *9*, 1546. (c) Atwood, J. L.; Barbour, L. J.; Jerga, A.; Schottel, B. L. *Science* **2002**, *298*, 1000. (d) Saha, B. K.; Nangia, A. *CrystEngComm* **2006**, *8*, 440. (e) Babu, N. J.; Reddy, L. S.; Aitipamula, S.; Nangia, A. *Chem., Asian J.* **2008**, *3*, 1122. (f) Lehmler, H.-J.; Robertson, L. W.; Parkin, S.; Brock, C. P. *Acta Crystallogr.* **2002**, *B58*, 140. (g) Brock, C. P. *Acta Crystallogr.* **2002**, *B58*, 1025. (h) Brock, C. P.; Duncan, L. L. *Chem. Mater.* **1994**, *6*, 1307. (i) Jetti, R. K. R.; Boese, R.; Sarma, J. A. R. P.; Reddy, L. S.; Vishweshwar, P.; Desiraju, G. R. *Angew. Chem., Int. Ed.* **2003**, *42*, 1963. (j) Sreekanth, B. R.; Vishweshwar, P.; Vyas, K. *Chem. Commun.* **2007**, 2375. (k) MacGillivray, L. R.; Zaworotko, M. J. *J. Chem. Cryst.* **1994**, *24*, 703.
- (4) (a) Colquhoun, H. M.; Williams, D. J.; Zhu, Z. *J. Am. Chem. Soc.* **2002**, *124*, 13346. (b) Cheney, M. L.; McManus, G. J.; Perman, J. A.; Wang, Z.; Zaworotko, M. J. *Cryst. Growth Des.* **2007**, *7*, 616. (c) Degenhardt, C., III; Shortell, D. B.; Adams, R. D.; Shimizu, K. D. *Chem. Commun.* **2000**, 929. (d) Degenhardt, C. F.; Lavin, J. M.; Smith, M. D.; Shimizu, K. D. *Org. Lett.* **2005**, *7*, 4079. (e) Rasberry, R. D.; Smith, M. D.; Shimizu, K. D. *Org. Lett.* **2008**, *13*, 2889. (f) Cagulada, A. M.; Hamilton, D. G. *J. Am. Chem. Soc.* **2009**, *131*, 902. (g) Jiang, Q.; Zhang, H.-Y.; Han, M.; Ding, Z.-J.; Liu, J. *Org. Lett.* **2010**, *12*, 1728. (h) Iwanaga, T.; Nakamoto, R.; Yasutake, M.; Shinmyozu, T. *Angew. Chem., Int. Ed.* **2006**, *45*, 3643.
- (5) (a) Barooah, N.; Sarma, R. J.; Baruah, J. B. *Cryst. Growth Des.* **2003**, *3*, 639. (b) Barooah, N.; Sarma, R. J.; Baruah, J. B. *CrystEngComm* **2006**, *8*, 608. (c) Baruah, J. B.; Karmakar, A.; Barooah, N. *CrystEngComm* **2008**, *10*, 151. (d) Gawronski, J.; Kaik, M.; Kwit, M.; Rychlewska, U. *Tetrahedron* **2006**, *62*, 7866. (e) Flamigni, L.; Johnston, M. R.; Giribabu, L. *Chem.—Eur. J.* **2002**, *8*, 3938.
- (6) (a) Mukhopadhyay, P.; Iwashita, Y.; Shirakawa, M.; Kawano, S.; Fujita, N.; Shinkai, S. *Angew. Chem., Int. Ed.* **2006**, *45*, 1592. (b) Pantos, G. D.; Pengo, P.; Sanders, J. K. M. *Angew. Chem., Int. Ed.* **2007**, *46*, 194. (c) Zhou, Q.-Z.; Jiang, X.-K.; Shao, X.-B.; Chen, G.-J.; Jia, M.-X.; Li, Z.-T. *Org. Lett.* **2003**, *5*, 1955. (d) Cairns, A. J.; Perman, J. A.; Wojtas, L.; Kravtsov, V. C.; Alkordi, M. H.; Eddaoudi, M.; Zaworotko, M. J. *J. Am. Chem. Soc.* **2008**, *130*, 1560. (e) Singh, D.; Baruah, J. B. *Tetrahedron Lett.* **2008**, *49*, 4374.
- (7) (a) Reger, D. L.; Debreczeni, A.; Horger, J. J.; Smith, M. D. *Cryst. Growth Des.* **2011**, *11*, 4068. (b) Reger, D. L.; Elgin, J. D.; Semeniuc, R. F.; Pellechia, P. J.; Smith, M. D. *Chem. Commun.* **2005**, 4068. (c) Reger, D. L.; Debreczeni, A.; Reinecke, B.; Rassolov, V.; Smith, M. D.; Semeniuc, R. F. *Inorg. Chem.* **2009**, *48*, 8911. (d) Reger, D. L.; Horger, J.; Smith, M. D.; Long, G. J. *Chem. Commun.* **2009**, 6219. (e) Reger, D. L.; Horger, J. J.; Smith, M. D.; Long, G. J.; Fernandez, G. *Inorg. Chem.* **2011**, *50*, 686.
- (8) (a) Bhogala, B. R.; Basavoju, S.; Nangia, A. *Cryst. Growth Des.* **2005**, *5*, 1683. (b) Bhogala, B. R.; Nangia, A. *Cryst. Growth Des.* **2003**, *3*, 547. (c) Blagden, N.; deMatas, M.; Gavan, P. T.; York, P. *Adv. Drug Delivery Rev.* **2007**, *59*, 617. (d) Biradha, K.; Zaworotko, M. J. *Cryst. Eng.* **1998**, *1*, 67. (e) Shan, N.; Bond, A. D.; Jones, W. *New J. Chem.* **2003**, *27*, 365. (f) Walsh, R. D. B.; Bradner, M. W.; Fleischman, S.; Morales, L. A.; Moulton, B.; Rodriguez-Hornedo, N.; Zaworotko, M. J. *Chem. Commun.* **2003**, 186. (g) Aakeröy, C. B.; Salmon, D. J. *CrystEngComm* **2005**, *7*, 439. (h) Sharma, C. V. K.; Broker, G. A.; Szulcowski, G. J.; Rogers, R. D. *Chem. Commun.* **2000**, 1023.
- (9) (a) Weyna, D. R.; Shattock, T.; Visweshwar, P.; Zaworotko, M. J. *Cryst. Growth Des.* **2009**, *9*, 1106. (b) Bhatt, P. M.; Ravindra, N. V.; Banerjee, R.; Desiraju, G. R. *Chem. Commun.* **2005**, 1073.
- (10) (a) Rajput, L.; Biradha, K. *Cryst. Growth Des.* **2009**, *9*, 40. (b) Lim, S.; Kim, H.; Selvapalam, N.; Kim, K. J.; Cho, S. J.; Seo, G.; Kim, K. *Angew. Chem., Int. Ed.* **2008**, *47*, 3352.
- (11) (a) Singh, D.; Bhattacharyya, P.; Baruah, J. B. *Cryst. Growth Des.* **2010**, *10*, 348. (b) Singh, D.; Baruah, J. B. *CrystEngComm* **2009**, *11*, 2688. (c) Singh, D.; Baruah, J. B. *Cryst. Growth Des.* **2011**, *11*, 768. (d) Singh, D.; Baruah, J. B. *Cryst. Growth Des.* **2012**, *12*, 2109.
- (12) (a) Silva, A. P. D.; Gunaratne, H. Q. N.; Gunlaugsson, T. *Tetrahedron Lett.* **1998**, *39*, 5077. (b) DiCesare, N.; Adhikari, D. P.; Heynekamp, J. J.; Heagy, M. D.; Lakowicz, J. R. *J. Fluoresc.* **2002**, *12*, 147. (c) Trupp, S.; Schweitzer, A.; Mohr, G. *J. Org. Biomol. Chem.* **2006**, *4*, 2965.
- (13) Sheldrick, G. M. *Acta Crystallogr.* **2008**, *A64*, 112.
- (14) (a) Zaworotko, M. J. *Chem. Commun.* **2001**, 1. (b) Etter, M. C.; Reutzel, S. M. *J. Am. Chem. Soc.* **1991**, *113*, 2586.
- (15) Alexiou, M. S.; Tychopoulos, V.; Ghorbanian, S.; Tyman, J. H. P.; Brown, R. G.; Brittain, P. I. *J. Chem. Soc. Perkin Trans. 2* **1990**, 837.
- (16) (a) Yang, J.-X.; Wang, X.-L.; Wang, X.-M.; Xu, L.-H. *Dyes Pigments* **2005**, *66*, 83. (b) Qian, X.; Tang, J.; Zhang, J.; Zhang, Y. *Dyes Pigments* **1994**, *25*, 109.
- (17) (a) Fu, X.-F.; Yue, Y.-F.; Guo, R.; Li, L.-L.; Sun, W.; Fang, C.-J.; Xu, C.-H.; Yan, C.-H. *CrystEngComm* **2009**, *11*, 2268. (b) Mizobe, Y.; Hinoue, T.; Yamamoto, A.; Hisaki, I.; Miyata, M.; Hasegawa, Y.; Tohnai, N. *Chem.—Eur. J.* **2009**, *15*, 8157. (c) Bindu, A.; Kelly, L. A. *J. Phys. Chem. B* **2003**, *107*, 12534.